Indian J Pure Appl Math (2024) 55:1365–1388
https://doi.org/10.1007/s13226-023-00444-9

ORIGINAL RESEARCH

Numerical dynamics of the Generalized Equal Width (GEW) wave equation in presence of high-order nonlinearity

Ali Başhan

Received: 27 April 2022 / Accepted: 2 June 2023 / Published online: 12 June 2023

Abstract In the present manuscript, Generalized Equal Width (GEW) wave equation which is an alternative model to shallow water wave with high-order nonlinearity is investigated. The GEW equation is solved for cubic, quartic and quintic nonlinear cases, separately. Solitary wave solution of the GEW equation for many applications and interaction of the two waves for two positive amplitudes, two negative amplitudes and one positive and one negative amplitude are solved. It is important to note that interaction of the two negative amplitude waves and interaction of the one positive and one negative wave solutions of the high-order GEW equation are firstly in this study examined. All applications are illustrated. The error norms for the solitary wave solution and the three invariants for all applications are calculated and reported. An illustrative comparison for the newly presented results displays the improvement of the present numerical solution. The rate of the convergence and CPU time is calculated for three different order nonlinear GEW equation.

Keywords GEW equation · Differential quadrature method · Finite difference method · Convergence

Mathematics Subject Classification 41A25 · 65M06 · 65D32 · 65D07

1 Introduction

Differential equations have a significant role to model natural phenomena. One of the famous shallow water wave is Korteweg-de Vries (KdV) equation. Morrison *et.al.* have investigated which is an alternative way of modelling of KdV equation and find solitary wave solutions that has equal wavelength [17]. The equal width wave (EW) equation has begun to attract many scientist due to its simple form as [26]

$$u_t + \varepsilon u u_x - \mu u_{xxt} = 0. \tag{1}$$

The EW equation is modified by using high order nonlinearity and called as modified equal width wave (MEW) equation. The MEW equation is usually given in the following form [7]

$$u_t + \varepsilon u^2 u_x - \mu u_{xxt} = 0. \tag{2}$$

After these works the EW equation is generalized and exact solutions are introduced [10,11,25]. The generalized equal width wave (GEW) equation is of the form

$$u_t + \varepsilon u^p u_x - \mu u_{xxt} = 0 \tag{3}$$

Communicated by G.D. Veerappa Gowda.

A. Başhan
Department of Mathematics, Zonguldak Bulent Ecevit University, 67100 zonguldak, Turkey
E-mail: alibashan@gmail.com

in which ε and μ stands for positive constants [25] and p is a positive integer [25]. Since, exact solutions of the GEW equation has limited availability, the scientist begin to obtain numerical solutions of the GEW equation. There are a few numerical studies related to GEW equation. Among others, Galerkin method [15], subdomain method [13,14], pseudospectral method [19], finite difference method [12] , collocation method [9,16,21,27] and Petrov-Galerkin method [22].

In this study, high order nonlinear GEW equation is solved by using two numerical methods. Classical finite difference method (FDM) has been utilized for solving the GEW equation by combination of the differential quadrature method (DQM) numerical solutions are improved. Bellman *et al* . [8] are firstly introduced the DQM. This efficient method is used for many scientific problems among others [1–6,8].

2 Quintic B-spline based DQM

DQM which is is put forward by R.E. Bellman and his colleagues *et al.* [8] has been started with the thought of integral quadrature. The main key of the DQM is to find out the required unknowns for the process of the discretization of the derivative related to space of any order [24] . We may express the fundamental formulae of the DQM as follows

$$\frac{d^{(r)}U}{dx^{(r)}}(x_i) = \sum_{j=1}^{N} c_{ij}^{(r)} U\left(x_j\right), \quad i = 1, 2, ..., N, \quad r = 1, 2, ..., N-1 \tag{4}$$

over the solution interval $[x_L, x_R]$ and mesh points distribution over the interval $x_L = x_1 < x_2 < \cdots < x_N = x_R$. R.E. Bellman and his colleagues which firstly presented the DQM, assuming that a function $U\left(x_j\right)$ is sufficiently smooth over the region $[x_L, x_R]$ [24].

The quintic B-splines $Q_m(x)$ are described as below:

$$Q_m(x) = \frac{1}{h^5}\begin{cases} s_1, & x \in [x_{m-3}, x_{m-2}], \\ s_1 - 6s_2, & x \in [x_{m-2}, x_{m-1}], \\ s_1 - 6s_2 + 15s_3, & x \in [x_{m-1}, x_m], \\ s_1 - 6s_2 + 15s_3 - 20s_4, & x \in [x_m, x_{m+1}], \\ s_1 - 6s_2 + 15s_3 - 20s_4 + 15s_5, & x \in [x_{m+1}, x_{m+2}], \\ s_1 - 6s_2 + 15s_3 - 20s_4 + 15s_5 - 6s_6, & x \in [x_{m+2}, x_{m+3}], \\ 0, & \text{otherwise} \end{cases}$$

where $s_1 = (x - x_{m-3})^5$, $s_2 = (x - x_{m-2})^5$, $s_3 = (x - x_{m-1})^5$, $s_4 = (x - x_m)^5$, $s_5 = (x - x_{m+1})^5$, $s_6 = (x - x_{m+2})^5$ and $h = x_m - x_{m-1}$ for all m [20]. The set of the B-splines $\{Q_{-1}, Q_0, \ldots, Q_{N+2}\}$ is for the functions which are defined on $[x_L, x_R]$ [24].

When we use Eq. (4) by using quintic B-spline basis functions for the 1st order derivative approach

$$\frac{\partial Q_m}{\partial x}(x_i) = \sum_{j=m-2}^{m+2} c_{i,j}^{(1)} Q_m\left(x_j\right), \quad i = 1, 2, ..., N, \quad m = -1, 0, \ldots, N+2, \tag{5}$$

we obtain an algebraic system that include $N + 8$ unknowns and $N + 4$ equations. For obtaining a solvable system we added four new equations that obtained by derivative of Eq. (5) for the $\{Q_{-1}, Q_0, Q_{N+1}, Q_{N+2}\}$ B-splines. So, the number of the equations and unknown terms are equalized. After the simplification steps we get a solvable new algebraic equation system

$$[E]\left[C_1^1\right] = \left[D_1^1\right] \tag{6}$$

where

$$[E]=\begin{bmatrix} 37 & 82 & 21 & & & & & & & \\ 8 & 33 & 18 & 1 & & & & & & \\ 1 & 26 & 66 & 26 & 1 & & & & & \\ & 1 & 26 & 66 & 26 & 1 & & & & \\ & & \ddots & \ddots & \ddots & \ddots & \ddots & & & \\ & & & & 1 & 26 & 66 & 26 & 1 & \\ & & & & & 1 & 26 & 66 & 26 & 1 \\ & & & & & & 1 & 18 & 33 & 8 \\ & & & & & & & 21 & 82 & 37 \end{bmatrix},$$

and

$$\left[C_1^1\right]=\left[c_{1,-1}^{(1)}\quad c_{1,0}^{(1)}\quad c_{1,1}^{(1)}\quad c_{1,2}^{(1)}\quad c_{1,3}^{(1)}\quad c_{1,4}^{(1)}\quad \cdots\quad c_{1,N+1}^{(1)}\quad c_{1,N+2}^{(1)}\right]^T$$

and

$$\left[D_1^1\right]=\left[-\frac{109}{2h}\quad -\frac{29}{h}\quad 0\quad \frac{50}{h}\quad \frac{5}{h}\quad 0\quad \cdots\quad 0\quad 0\right]^T.$$

For the other points, the weights can be computed in the same manner. For the grid points $x_k, 2 \le k \le N-1$ we got the algebraic equation system:

$$[E]\left[C_k^1\right]=\left[D_k^1\right] \tag{7}$$

where

$$\left[C_k^1\right]=\left[c_{k,-1}^{(1)}\ \cdots\ c_{k,k-3}^{(1)}\ c_{k,k-2}^{(1)}\ c_{k,k-1}^{(1)}\ c_{k,k}^{(1)}\ c_{k,k+1}^{(1)}\ c_{k,k+2}^{(1)}\ c_{k,k+3}^{(1)}\ \cdots\ c_{k,N+2}^{(1)}\right]^T$$

and

$$\left[D_k^1\right]=\left[0\quad \cdots\quad 0\quad -\frac{5}{h}\quad -\frac{50}{h}\quad 0\quad \frac{50}{h}\quad \frac{5}{h}\quad 0\quad \cdots\quad 0\right]^T.$$

The same process is applied to the last grid point x_N, by the same process, for the determination weighting coefficients $c_{N,j}^{(1)},\quad j=-1,0,\ldots,N+2$ we got the algebraic equation system:

$$[E]\left[C_N^1\right]=\left[D_N^1\right] \tag{8}$$

where

$$\left[C_N^1\right]=\left[c_{N,-1}^{(1)}\quad c_{N,0}^{(1)}\quad \cdots\quad c_{N,N-3}^{(1)}\quad c_{N,N-2}^{(1)}\quad c_{N,N-1}^{(1)}\quad c_{N,N}^{(1)}\quad c_{N,N+1}^{(1)}\quad c_{N,N+2}^{(1)}\right]^T$$

and

$$\left[D_N^1\right]=\left[0\quad 0\quad \cdots\quad 0\quad -\frac{5}{h}\quad -\frac{50}{h}\quad 0\quad \frac{29}{h}\quad \frac{109}{2h}\right]^T.$$

The same algebraic process has been implemented to find 2nd order weighting coefficients.

3 Discretization process

In this section, the GEW equation (3) is going to be discritized. An effective type of the FDM that is Crank-Nicolson type technique is applied to Eq. (3) as follows,

$$\frac{U^{n+1}-U^{n}}{\Delta t}+\varepsilon.\frac{(U^{p}U_{x})^{n+1}+(U^{p}U_{x})^{n}}{2}-\mu\frac{U_{xx}^{n+1}-U_{xx}^{n}}{\Delta t}=0. \tag{9}$$

Eq. (9) is reorganized and the following repetitive scheme is found out

$$2U^{n+1}+\varepsilon\Delta t\left(U^{p}U_{x}\right)^{n+1}-2\mu U_{xx}^{n+1}=2U^{n}-\varepsilon\Delta t\left(U^{p}U_{x}\right)^{n}-2\mu U_{xx}^{n}. \tag{10}$$

To obtain a solvable equation system Rubin and Graves type linearizing technique [23] is used for different order of nonlinearity. Rubin and Graves type linearizing technique is given as [23]

$$(u_{i}m_{i})^{n+1}=u_{i}^{n}m_{i}^{n+1}+u_{i}^{n+1}m_{i}^{n}-u_{i}^{n}m_{i}^{n}.$$

For example, when $p=2$ is chosen and nonlinear terms are vanished

$$2U^{n+1}+\varepsilon\Delta t\left(U^{n}\right)^{2}U_{x}^{n+1}+2\varepsilon\Delta tU^{n}U_{x}^{n}U^{n+1}-2\mu U_{xx}^{n+1}=2U^{n}+\varepsilon\Delta t\left(U^{n}\right)^{2}U_{x}^{n}-2\mu U_{xx}^{n}, \tag{11}$$

obtained. Some of the terms to be used in Eq. (11) are redefined as follows for easy reference

$$\begin{aligned} A_{i}^{n}&=\sum_{j=1}^{N}c_{ij}^{(1)}U_{j}^{n}=U_{x_i}^{n}, \quad B_{i}^{n}=\sum_{j=1}^{N}c_{ij}^{(2)}U_{j}^{n}=U_{xx_i}^{n},\\ U_{x_i}^{n+1}&=\sum_{j=1}^{N}c_{ij}^{(1)}U_{j}^{n+1}, \quad U_{xx_i}^{n+1}=\sum_{j=1}^{N}c_{ij}^{(2)}U_{j}^{n+1}, \end{aligned} \tag{12}$$

where A_i^n and B_i^n are the 1^{st} and 2^{nd} order derivative approximations for function U at the n^{th} time level on points x_i, respectively. Via substituting the definitions given in (12) into Eq. (11) and rearranging at the every node, the following equality results in

$$\begin{aligned} &\left[2+\varepsilon\Delta t\left(\left(U_{i}^{n}\right)^{2}c_{ii}^{(1)}+2U_{i}^{n}A_{i}^{n}\right)-2\mu c_{ii}^{(2)}\right]U_{i}^{n+1}+\\ &\left[\sum_{j=1,i\neq j}^{N}\left(\varepsilon\Delta t\left(U_{i}^{n}\right)^{2}c_{ij}^{(1)}-2\mu c_{ij}^{(2)}\right)U_{j}^{n+1}\right]\\ &=L_{i}^{n} \end{aligned}$$

where

$$L_{i}^{n}=2U_{i}^{n}+\varepsilon\Delta t\left(U_{i}^{n}\right)^{2}A_{i}^{n}-2\mu B_{i}^{n},\ \text{for } i=1(1)N.$$

The equation system in the matrix form can be reorganized as below

$$\begin{bmatrix} H_{1,1} & H_{1,2} & \cdots & H_{1,N}\\ H_{2,1} & H_{2,2} & \cdots & H_{2,N}\\ \vdots & \vdots & \ddots & \vdots\\ H_{N-1,1} & H_{N-1,2} & \cdots & H_{N-1,N}\\ H_{N,1} & H_{N,2} & \cdots & H_{N,N} \end{bmatrix}\begin{bmatrix} U_{1}^{n+1}\\ U_{2}^{n+1}\\ \vdots\\ U_{N-1}^{n+1}\\ U_{N}^{n+1} \end{bmatrix}=\begin{bmatrix} L_{1}^{n}\\ L_{2}^{n}\\ \vdots\\ L_{N-1}^{n}\\ L_{N}^{n} \end{bmatrix}. \tag{13}$$

Next, the conditions given at the boundaries are applied to the (13) and for obtaining a solvable system the first and last equations are eliminated. So,

$$\begin{bmatrix} H_{2,2} & H_{2,3} & \cdots & H_{2,N-1} \\ H_{3,2} & H_{3,3} & \cdots & H_{3,N-1} \\ \vdots & \vdots & \ddots & \vdots \\ H_{N-1,2} & H_{N-1,3} & \cdots & H_{N-1,N-1} \end{bmatrix} \begin{bmatrix} U_2^{n+1} \\ U_3^{n+1} \\ \vdots \\ U_{N-1}^{n+1} \end{bmatrix} = \begin{bmatrix} L_2^n - H_{2,1}U_1^{n+1} - H_{2,N}U_N^{n+1} \\ L_3^n - H_{3,1}U_1^{n+1} - H_{3,N}U_N^{n+1} \\ \vdots \\ L_{N-1}^n - H_{N-1,1}U_1^{n+1} - H_{N-1,N}U_N^{n+1} \end{bmatrix}$$

is obtained. For the higher-order GEW equation a similar process is implemented and then finally the obtained system has been solved by means of Gauss elimination method.

4 Numerical applications

In order to test the performance of the newly proposed method, the error norms L_2 and L_∞ are used:

$$L_2 = \left(h \sum_{J=1}^{N} \left| u_j - U_j \right|^2 \right)^{1/2}, \qquad L_\infty = \max_{1 \le j \le N} \left| u_j - U_j \right|.$$

Olver has presented the formulae of these three invariants for EW and RLW equations [18]. They are used corresponding to mass, momentum and energy, respectively for GEW equation as below

$$I_1 = \int_{-\infty}^{\infty} U dx, \quad I_2 = \int_{-\infty}^{\infty} \left(U^2 + \mu U_x^2 \right) dx, \quad I_3 = \int_{-\infty}^{\infty} U^{p+2} dx.$$

The convergence ratio has been computed with the following formulae

$$ROC \simeq \frac{\ln \left(Error\,(N_2)\,/ Error\,(N_1) \right)}{\ln \left(N_1 / N_2 \right)}.$$

All of the applications are performed on PC which has Intel(R) Core(TM) i7-4770 CPU @ 3.40GHz processor and 16 GB RAM.

4.1 Single solitary wave solutions

Exact solution of the GEW equation for the single solitary wave is firstly given by Hamdi *et.al.* [10] as follows

$$U(x,t) = A \left(\operatorname{sech} \left[\delta \left(x - x_0 - ct \right) \right] \right)^{2/p}, \tag{14}$$

in which the amplitude is given as $A = \left(\frac{c(p+1)(p+2)}{2\varepsilon} \right)^{1/p}$ and $\delta = \sqrt{\frac{p^2}{4\mu}}$.

The initial condition is obtained from exact solution as

$$U(x,0) = A \left(\operatorname{sech} \left[\delta \left(x - x_0 \right) \right] \right)^{2/p}$$

and the boundary conditions require $U \to 0$ for $x \to \pm\infty$. In this part, three different order of the nonlinearity is investigated.

A.1. First of all, for the solitary wave test problem of the cubic nonlinear GEW equation $p = 2$ and great amplitude $A = 1$ are used. The constant parameters are chosen as $c = 0.5$, $\varepsilon = 3$, $\mu = 1$, $x_0 = 30$ over the solution domain $[0, 80]$. The present results are obtained for three different time increment as $\Delta t = 0.2$, $\Delta t = 0.1$ and $\Delta t = 0.05$ to compare with those of earlier works [12,13,15,19]. Comparison of the present error norms L_2 and L_∞ and the three invariants with earlier works [12–16,19,27] are given in Table 1. The present error norms are found to be less than all of the given methods except subdomain method [14] and collocation method [16,27]. This application displays the significant improvement of the classical FDM with combination of the DQM and FDM. The present invariants are observed nearly unchanged. Numerical simulation of the single

Table 1 Single solitary wave: $p = 2$, $A = 1$, $x \in [0, 80]$.

Method	Δt	N	t	L_2	L_∞	I_1	I_2	I_3
Present	0.2	501	0	0.0000000	0.0000000	3.1415930	2.6666670	1.3333330
			5	0.0066613	0.0043096	3.1415990	2.6664070	1.3330720
			10	0.0138224	0.0087892	3.1416100	2.6661410	1.3328060
			15	0.0213241	0.0134667	3.1416040	2.6658500	1.3325160
			20	0.0290683	0.0181461	3.1416030	2.6655700	1.3322350
Present	0.1	701	0	0.0000000	0.0000000	3.1415920	2.6666680	1.3333340
			5	0.0016751	0.0010831	3.1415790	2.6665970	1.3332640
			10	0.0034518	0.0021990	3.1415900	2.6665840	1.3332510
			15	0.0052715	0.0033142	3.1416310	2.6666150	1.3332820
			20	0.0070704	0.0044150	3.1416540	2.6666250	1.3332900
Present	0.05	781	0	0.0000000	0.0000000	3.1415920	2.6666670	1.3333330
			5	0.0004099	0.0002617	3.1416130	2.6666840	1.3333510
			10	0.0007933	0.0004886	3.1416750	2.6667900	1.3334580
			15	0.0011462	0.0007040	3.1416790	2.6667770	1.3334440
			20	0.0015069	0.0009289	3.1416760	2.6667600	1.3334280
Gal. [15]	0.2	801	20	0.0380303	0.0262900	3.1589605	2.6902580	1.3570299
Subd. [13]	0.2	801	20	0.0544214	0.0360834	3.1251634	2.6447698	1.3115241
Subd. [14]	0.2	801	20	0.0201403	0.0124633	3.1415870	2.6666621	1.3333284
P.S. [19]	0.2	801	20	0.0291111	0.0182768	3.1415927	2.6655435	1.3322083
FDM [12]	0.1	801	20	0.014996	0.009788	-	-	-
FDM [12]	0.05	801	20	0.009863	0.006669	-	-	-
Coll. [27]First	0.2	801	20	0.0513210	0.0341675	3.1250343	2.6445829	1.3113394
Coll. [27]Second	0.2	801	20	0.0167509	0.0102639	3.1416722	2.6669051	1.3335718
Coll. [16]First	0.2	801	20	0.0167182	0.0104012	3.1415854	2.6666604	1.3333266
Coll. [16]Second	0.2	801	20	0.0170896	0.0105008	3.1415858	2.6666600	1.3333267

Table 2 A.1. The amplitude and location of the single solitary wave: $p = 2$, $A = 1$, $x \in [0, 80]$.

Method	Δt	N	t	x	$U(Num)$	$U(Ana)$
Present	0.05	781	0	30.05128	0.99869	0.99869
			5	32.51282	0.99993	0.99992
			10	34.97436	0.99974	0.99967
			15	37.53846	0.99925	0.99926
			20	40.00000	1.00003	1.00000

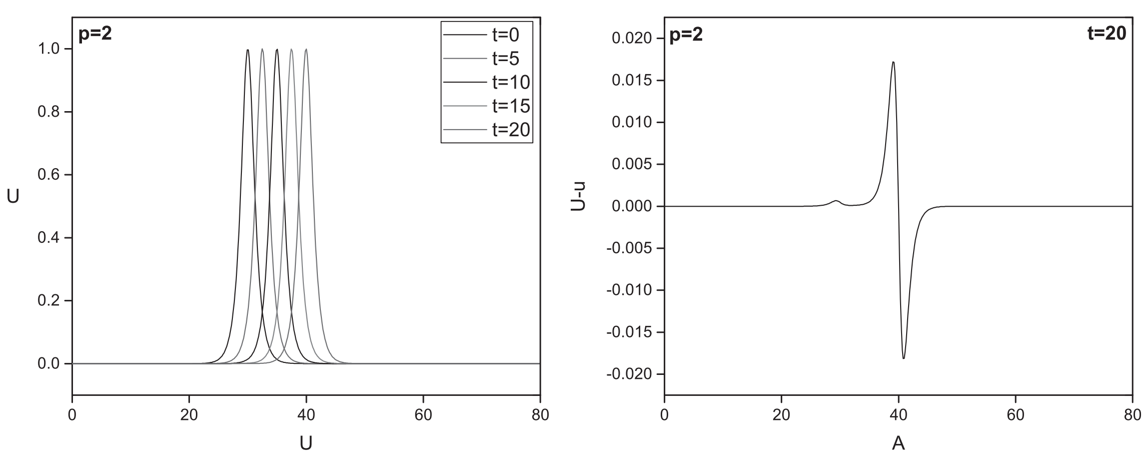

Fig. 1 A.1. Single solitary wave and maximum error: $p = 2$, $A = 1$ $\Delta t = 0.2$.

Table 3 A.2. Single solitary wave: $p = 2$, $A = 0.25$, $x \in [0, 80]$, $\Delta t = 0.2$.

Method	N	t	$L_2 \times 10^5$	$L_\infty \times 10^5$	I_1	I_2	I_3
Present	731	0	0.00000	0.00000	0.7853982	0.1666666	0.0052083
		5	0.13651	0.13660	0.7853960	0.1666652	0.0052082
		10	0.08841	0.08110	0.7853968	0.1666659	0.0052083
		15	0.11388	0.10463	0.7853961	0.1666657	0.0052083
		20	0.08186	0.06668	0.7853993	0.1666671	0.0052084
Gal. [15]	801	20	7.83378	4.44850	0.7853968	0.1666663	0.0052083
P.S. [19]	400	20	0.16098	0.10082	0.7853981	0.1666666	0.0052083
P.S. [19]	250	20	0.16858	0.11613	0.7853982	0.1666667	0.0052083
FDM [12]	801	20	27.0	25.7	0.785398	0.166666	0.005208
Coll. [21]		20	19.5887	17.4433	-	-	-
Coll. [9]	801	20	15.6953	20.2147	0.7852864	0.1665818	0.0052060
Coll. [27] First	801	20	0.14404	0.10853	0.7853965	0.1666663	0.0052083
Coll. [27] Second	801	20	0.13526	0.09151	0.7853966	0.1666664	0.0052083
Coll. [16] First	801	20	0.13336	0.08399	0.7853965	0.1666663	0.0052083
Coll. [16] Second	801	20	0.12775	0.06887	0.7853965	0.1666663	0.0052083
P-G. [22]	801	20	0.25017	0.27516	0.785398	0.166669	0.0052082

Table 4 A.2. The rate of convergence and CPU time: $p = 2$, $A = 0.25$, $x \in [0, 80]$, $\Delta t = 0.2$, $t= 20$.

N	$L_2 \times 10^5$	ROC	$L_\infty \times 10^5$	ROC	CPU time (sec.)
101	306.19383	-	228.77072	-	0.672
201	9.64762	5.02410	11.78712	4.30947	6.828
401	0.48011	4.34435	0.59288	4.32888	50.250
601	0.21451	1.99108	0.23470	2.29018	171.844
731	0.08186	4.91959	0.06668	6.42637	297.125

solitary wave is depicted in Figure 1. Both the amplitude and the shape of the wave are almost conserved during the simulation time. This situation may be observed at amplitude and location values of the solitary wave given in Table 2. The highest value of error at the final of the simulation is plotted in Figure 1. It is clear to say that the error values are zero at the left and right boundaries of the solution domain.

A.2. Secondly, using $p = 2$ and a smaller amplitude value $A = 0.25$, new solutions have been sought. For this case, $c = 1/32$, $\varepsilon = 3$, $\mu = 1$, $x_0 = 30$, are used over the solution domain $[0, 80]$. The new results have been found out for $\Delta t = 0.2$ to display the comparative analysis with earlier works [9,12,15,16,19,21,22,27]. The error norms L_2 and L_∞ and the three invariants are given in Table 3 with some of the other existing results [9,12,15,16,19,21,22,27]. The present error norms are smaller than those of earlier works [9,12,15,16,19,21, 22,27] at the end of the simulation. An improvement in the newly found numerical results can be clearly seen in this comparative situation. The present invariants are recorded almost constant. The rate of the convergence, the error norms and CPU time values are given in Table 4. By increasing of the number of the grid points inversely proportional error norms decreased.

B.1. For increasing the order of the nonlinearity from $p = 2$ to the $p = 3$, two different applications are investigated. Firstly, a great amplitude $A = 1$ is chosen. In this present case, $c = 0.3$, $\varepsilon = 3$, $\mu = 1$, $x_0 = 30$, are used over the solution domain $[0, 80]$. The present results are obtained for $\Delta t = 0.2$ and are compared with some of the earlier studies [13–15]. The error norms L_2 and L_∞ and the three invariants are given in Table 5 with some of the other available ones [13–16,27]. The present error norms are smaller than earlier works except collocation method [16,27] at the end of the simulation. The present invariants are recorded to be nearly unchanged. Numerical illustration of the single solitary wave for the great amplitude is plotted in Figure 2. The shape and amplitude are conserved during the simulation run. Maximum error value in the final of the run simulation has been plotted in Figure 2. It is clearly seen that at the left boundary and right boundary the error values are zero.

B.2. The second application related to the higher order nonlinearity $p = 3$, smaller amplitude $A = 0.15$ is chosen. For this case, $c = 0.001$, $\varepsilon = 3$, $\mu = 1$, $x_0 = 30$, have been utilized throughout the solution region $[0, 80]$. The present results are obtained for $\Delta t = 0.2$ to show an analysis with those of the previous studies [15,21] in a comparative way. The error norms L_2 and L_∞ and the three invariants are given in Table 6 with some of the other existing results [15,21]. The present error norms are smaller than earlier works [15,21] at the

Table 5 B.1. Single solitary wave: $p = 3$, $A = 1$, $x \in [0, 80]$, $\Delta t = 0.2$.

Method	N	t	L_2	L_∞	I_1	I_2	I_3
Present	731	0	0.0000000	0.0000000	2.804363	2.463914	0.9855653
		5	0.0033743	0.0023512	2.804366	2.463753	0.9854035
		10	0.0069400	0.0048000	2.804391	2.463628	0.9852794
		15	0.0106903	0.0073461	2.804404	2.463476	0.9851275
		20	0.0145766	0.0099490	2.804428	2.463341	0.9849923
Gal. [15]	801	20	0.0165563	0.0137045	2.818739	2.485224	1.0070200
Subd. [13]	801	20	0.0460246	0.0333820	2.791106	2.444400	0.9661645
Subd. [14]	801	20	0.0150331	0.0099935	2.804356	2.463908	0.9855599
Coll. [27]First	801	20	0.0080147	0.0053823	2.804357	2.463908	0.9855602
Coll. [27]Second	801	20	0.0070855	0.0048047	2.804294	2.463908	0.9854011
Coll. [16]First	801	20	0.0080099	0.0053773	2.804357	2.463908	0.9855602
Coll. [16]Second	801	20	0.0070809	0.0048035	2.804294	2.463749	0.9854012

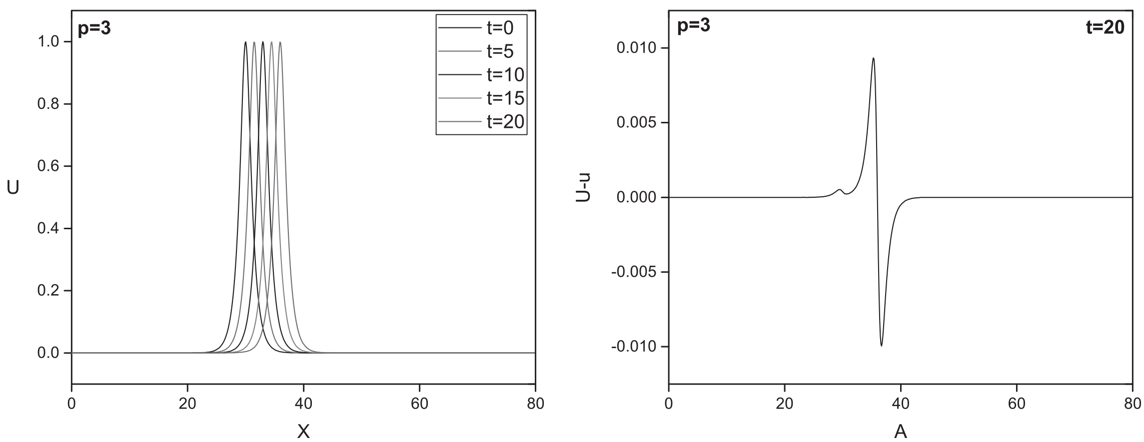

Fig. 2 B.1. Single solitary wave and maximum error: $p = 3$, $A = 1$, $\Delta t = 0.2$.

Table 6 B.2. Single solitary wave: $p = 3$, $A = 0.15$, $x \in [0, 80]$, $\Delta t = 0.2$.

Method	N	t	$L_2 \times 10^6$	$L_\infty \times 10^6$	I_1	I_2	$I_3 \times 10^4$
Present	451	0	0.00000000	0.00000000	0.4189162	0.05498081	0.7330779
		5	0.16113336	0.18102764	0.4189165	0.05498079	0.7330769
		10	0.22642645	0.28116422	0.4189161	0.05498075	0.7330758
		15	0.52117994	0.51911867	0.4189151	0.05498060	0.7330708
		20	0.33472689	0.32575615	0.4189162	0.05498088	0.7330800
Gal. [15]	801	20	2.82488132	1.83291025	0.4189154	0.0549805	0.733
Coll. [21]	801	20	514.9677	320.60590	-	-	-

end of the simulation. The present invariants are recorded to be nearly unchanged. The rate of the convergence, the error norms and CPU time values are given in Table 7. By an increase in the number of grid points inversely proportional error norms decreased.

C.1. For increasing the order nonlinearity from $p = 3$ to the $p = 4$, two different applications are investigated. Firstly, a great amplitude $A = 1$ is chosen. For this case, $c = 0.2$, $\varepsilon = 3$, $\mu = 1$, $x_0 = 30$, have been utilized throughout the solution range [0, 80]. The new results have been found out for $\Delta t = 0.2$ for comparison with earlier works [13–16,27]. The error norms L_2 and L_∞ and the three invariants are given in Table 8 with other existing results [13–16,27]. The present error norm are smaller than earlier works except collocation method [16,27] at the end of the simulation. The present invariants are observed nearly unchanged. Numerical illustration of the single solitary wave for the great amplitude is plotted in Figure 3. Both of the amplitude and shape are conserved through the run simulation during the simulation run. Maximum error value at the end of the simulation is plotted in Figure 3. It is clearly seen that at the both of the boundary sides the error values are zero and the highest value of the error has been observed near the peak of the wave.

Table 7 B.2. The rate of convergence and CPU time: $p = 3$, $A = 0.15$, $x \in [0, 80]$, $\Delta t = 0.2$ t= 20.

N	$L_2 \times 10^6$	ROC	$L_\infty \times 10^6$	ROC	CPU time (sec.)
101	108.93949	-	84.08462	-	0.656
151	38.56002	2.58250	47.71554	1.40881	2.641
181	2.94115	5.06405	3.86854	4.94395	4.719
201	0.87491	3.61561	1.23039	3.41614	6.516
251	0.33473	3.83274	0.32576	5.30126	9.969

Table 8 C.1. Single solitary wave: $p = 4$, $A = 1$, $x \in [0, 80]$, $\Delta t = 0.2$.

Method	N	t	L_2	L_∞	I_1	I_2	I_3
Present	751	0	0.0000000	0.0000000	2.622056	2.356194	0.7853981
		5	0.0018316	0.0013248	2.622070	2.356117	0.7853221
		10	0.0037303	0.0027095	2.622077	2.356036	0.7852393
		15	0.0057341	0.0041580	2.622089	2.355957	0.7851607
		20	0.0078180	0.0056366	2.622103	2.355878	0.7850807
Gal. [15]	801	20	0.0089061	0.0082199	2.632783	2.373003	0.8023383
Subd. [13]	801	20	0.0375343	0.0287549	2.612205	2.340813	0.7701119
Subd. [14]	801	20	0.0142772	0.0090800	2.622045	2.356183	0.7853869
Coll. [27]First	801	20	0.0042169	0.0029795	2.622050	2.356190	0.7853939
Coll. [27]Second	801	20	0.0033908	0.0024703	2.621928	2.355932	0.7851364
Coll. [16]First	801	20	0.0042083	0.0029695	2.622050	2.356190	0.7853939
Coll. [16]Second	801	20	0.0034148	0.0024936	2.621921	2.355909	0.7851130

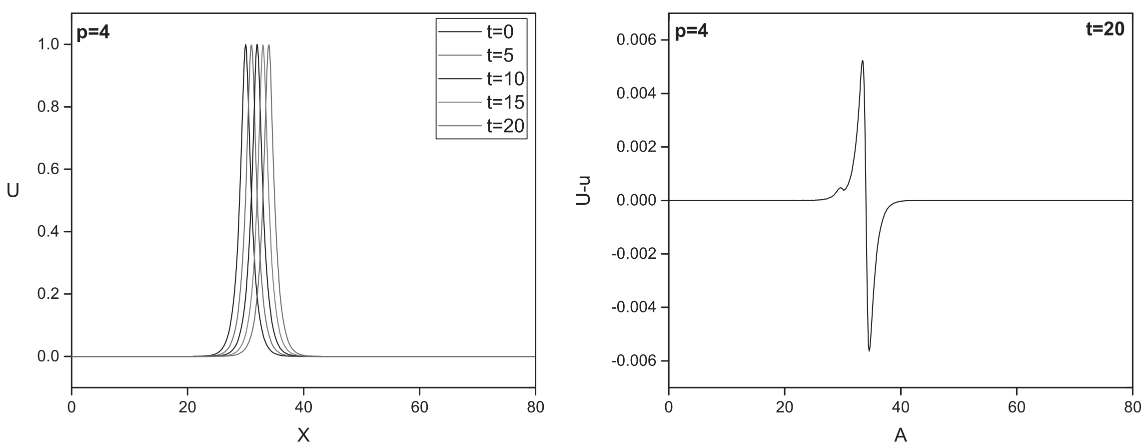

Fig. 3 C.1. Single solitary wave and maximum error: $p = 4$, $A = 1$, $\Delta t = 0.2$.

C.2. The second application is related to the higher order nonlinearity $p = 4$, smallest amplitude $A = 0.1$ is chosen. For this case, $c = 0.00002$, $\varepsilon = 3$, $\mu = 1$, $x_0 = 30$, are used over the solution domain [0, 80]. The new results have been found out for time increment $\Delta t = 0.2$. The error norms L_2 and L_∞ and the three invariants are given in Table 9. The present error norm L_2 is 1.36×10^{-7}, and the error norm L_∞ is 1.35×10^{-7} at the end of the simulation. This application is firstly given in the present study. So, numerical results can not compared with any earlier work. The present invariants are observed to be nearly unchanged. The convergence ratio for the error norms and CPU time values are given in Table 10. By increasing the number of the grid points inversely proportional error norms are decreased. Comparison of the CPU time values for single solitary wave is given in Table 11.

4.2 Interaction of the two solitary waves for different cases

The interaction of the two solitary waves are investigated for two positive amplitude, two negative amplitude and one positive and one negative amplitude waves for cubic, quartic and quintic nonlinear forms of the GEW equation.

Table 9 C.2. Single solitary wave: $p = 4$, $A = 0.1$, $x \in [0, 80]$, $\Delta t = 0.2$.

Method	N	t	$L_2 \times 10^7$	$L_\infty \times 10^7$	I_1	I_2	$I_3 \times 10^5$
Present	661	0	0.0000000	0.0000000	0.2622056	0.0235619	0.0785398
		5	1.8996765	1.3829922	0.2622057	0.0235619	0.0785395
		10	3.6933885	3.0476562	0.2622064	0.0235620	0.0785402
		15	4.5598500	2.8559919	0.2622068	0.0235620	0.0785408
		20	1.3604376	1.3528486	0.2622056	0.0235619	0.0785397

Table 10 C.2. The rate of convergence and CPU time: $p = 4$, $A = 0.1$, $x \in [0, 80]$, $\Delta t = 0.2$ at t= 20.

N	$L_2 \times 10^6$	ROC	$L_\infty \times 10^6$	ROC	CPU time (sec.)
51	25.81970	-	20.10325	-	0.047
101	3.06375	3.11944	2.11118	3.29819	0.688
201	0.70784	2.12905	0.82950	1.35745	6.516
401	0.48181	0.55696	0.35358	1.23464	49.859
661	0.13604	2.53025	0.13528	1.92232	240.250

Table 11 A, B, C. Comparison of the CPU time values for single solitary wave

p	c	A	Δt	N	T_{Final}	CPU time (sec.)
2	0.5	1	0.2	201	20	6.703
3	0.3	1	0.2	201	20	6.516
4	0.2	1	0.2	201	20	6.438
2	0.5	1	0.2	401	20	48.984
3	0.3	1	0.2	401	20	48.922
4	0.2	1	0.2	401	20	49.141
2	0.5	1	0.2	601	20	172.406
3	0.3	1	0.2	601	20	171.031
4	0.2	1	0.2	601	20	170.844

D. In this part, numerical solutions of the interactions of the two different waves for cubic nonlinear GEW equation are investigated.

D.1. Firstly, numerical solutions of the interaction of the two positive amplitudes for cubic nonlinear GEW equation is investigated. The condition given at the initial time is selected as follows

$$U(x, 0) = A_1 (\sec\mathrm{h} [\delta (x - x_1)])^{2/p} + A_2 (\sec\mathrm{h} [\delta (x - x_2)])^{2/p} \tag{15}$$

where amplitude is $A_k = \left(\frac{c_k(p+1)(p+2)}{2\varepsilon}\right)^{1/p}$ $(k = 1,\ 2)$ and $\delta = \sqrt{\frac{p^2}{4\mu}}$. To observe the interaction of the two positive amplitude waves for cubic nonlinearity, the fixed coefficients have been selected as follows $p = 2$, $\varepsilon = 3$, $\mu = 1$, $x_1 = 15$, $x_2 = 30$, $c_1 = 0.5$, $c_2 = 0.125$. So, the great amplitude value is $A_1 = 1$ chosen and small amplitude value is $A_2 = 0.5$ chosen. Numerical solution investigated over the solution domain [0, 80] and simulation run up to time $t = 60$. The numerical solution is obtained for $\Delta t = 0.05$ and $N = 201$. Numerical invariants are given in Table 12. The three invariants are seen to be nearly unchanged during the simulation. The interaction of the waves is illustrated and given in Figure 4. In Figure 4, the two solitary waves are seen at the end of the simulation with small differences in terms of initial position.

D.2. Secondly, numerical solutions of the interaction of the two negative amplitudes for cubic nonlinear GEW equation is investigated. The condition given at the initial time is selected as follows

$$U(x, 0) = -A_1 (\sec\mathrm{h} [\delta (x - x_1)])^{2/p} - A_2 (\sec\mathrm{h} [\delta (x - x_2)])^{2/p} \tag{16}$$

where amplitude is $A_k = \left(\frac{c_k(p+1)(p+2)}{2\varepsilon}\right)^{1/p}$ $(k = 1,\ 2)$ and $\delta = \sqrt{\frac{p^2}{4\mu}}$. To observe the interaction of the two negative amplitude waves for cubic nonlinearity, the fixed coefficients have been selected as follows $p = 2$, $\varepsilon = 3$, $\mu = 1$, $x_1 = 15$, $x_2 = 30$, $c_1 = 0.5$, $c_2 = 0.125$. So, the great amplitude value is $A_1 = 1$ chosen and small amplitude value is $A_2 = 0.5$ chosen. Numerical solution investigated over the solution domain [0, 80] and simulation run up to time $t = 60$. The numerical solution is obtained for $\Delta t = 0.05$ and $N = 201$. The

Table 12 D. Interaction of the two solitary waves: $p = 2$, $x \in [0, 80]$, $\Delta t = 0.05$, $N = 201$.

	A_1=1, A_2=0.5			$A_1 = -1$, $A_2 = -0.5$			A_1=1, $A_2 = -0.5$		
t	I_1	I_2	I_3	I_1	I_2	I_3	I_1	I_2	I_3
0	4.71239	3.33329	1.41667	− 4.71239	3.33329	1.41667	1.57080	3.33328	1.41666
10	4.71227	3.33326	1.41664	− 4.71227	3.33326	1.41664	1.57069	3.33328	1.41666
20	4.71217	3.33325	1.41663	− 4.71217	3.33325	1.41663	1.57057	3.33327	1.41665
30	4.71206	3.33321	1.41652	− 4.71206	3.33321	1.41652	1.57047	3.33326	1.41678
40	4.71196	3.33322	1.41659	− 4.71196	3.33322	1.41659	1.57085	3.33357	1.42038
50	4.71186	3.33323	1.41664	− 4.71186	3.33323	1.41664	1.57022	3.33319	1.41660
60	4.71174	3.33323	1.41662	− 4.71174	3.33323	1.41662	1.57007	3.33317	1.41663

numerical values of the calculated invariants are presented in Table 12. The three invariants are seen to be nearly unchanged during the simulation. The interaction of the waves is illustrated and given in Figure 5. In Figure 5, the two solitary waves are seen in the final of the simulation having small differences according to initial position.

D.3. Thirdly, numerical solutions of the interaction of the one positive and one negative amplitudes for cubic nonlinear GEW equation is investigated. The condition given at the initial time is selected as follows

$$U(x,0) = A_1\,(\operatorname{sech}[\delta\,(x-x_1)])^{2/p} - A_2\,(\operatorname{sech}[\delta\,(x-x_2)])^{2/p} \tag{17}$$

where amplitude is $A_k = \left(\frac{c_k(p+1)(p+2)}{2\varepsilon}\right)^{1/p}$ $(k = 1,\ 2)$ and $\delta = \sqrt{\frac{p^2}{4\mu}}$. To observe the interaction of the two positive amplitude waves for cubic nonlinearity, the fixed coefficients have been selected as follows $p = 2$, $\varepsilon = 3$, $\mu = 1$, $x_1 = 15$, $x_2 = 30$, $c_1 = 0.5$, $c_2 = 0.125$. So, the great amplitude value is $A_1 = 1$ chosen and small amplitude value is $A_2 = 0.5$ chosen. Numerical solution investigated over the solution domain [0, 80] and simulation run up to time $t = 60$. The numerical solution is obtained for $\Delta t = 0.05$ and $N = 201$. Numerical invariants are given in Table 12. The three invariants are seen to be nearly unchanged during the simulation. The interaction of the waves is illustrated and given in Figure 6. In Figure 6, the two solitary waves are seen at the end of the simulation with small differences according to initial position.

E. In this part, numerical solutions of the interactions of the two different waves for quartic nonlinear GEW equation are investigated.

E.1. Firstly, numerical solutions of the interaction of the two positive amplitudes for quartic nonlinear GEW equation is investigated. The condition given at the initial time is selected as follows

$$U(x,0) = A_1\,(\operatorname{sech}[\delta\,(x-x_1)])^{2/p} + A_2\,(\operatorname{sech}[\delta\,(x-x_2)])^{2/p} \tag{18}$$

where amplitude is $A_k = \left(\frac{c_k(p+1)(p+2)}{2\varepsilon}\right)^{1/p}$ $(k = 1,\ 2)$ and $\delta = \sqrt{\frac{p^2}{4\mu}}$. To observe the interaction of the two positive amplitude waves for quartic nonlinearity, values of the constant parameters are chosen as $p = 3$, $\varepsilon = 3$, $\mu = 1$, $x_1 = 15$, $x_2 = 30$, $c_1 = 0.3$, $c_2 = 0.0375$. So, the great amplitude value is $A_1 = 1$ chosen and small amplitude value is $A_2 = 0.5$ chosen. Numerical solution investigated over the solution domain [0, 80] and simulation run till $t = 100$. The numerical solution is obtained for $\Delta t = 0.05$ and $N = 801$. Numerical invariants are given in Table 13. The three invariants are seen to be nearly unchanged during the simulation. The interaction of the waves is illustrated and given in Figure 7. In Figure 7, the two solitary waves are seen with two small wavelets in the final of the run simulation. The present condition may be explained with the increasing of the order of the nonlinearity.

E.2. Secondly, numerical solutions of the interaction of the two negative amplitudes for quartic nonlinear GEW equation is investigated. The condition given at the initial time is selected as follows

$$U(x,0) = -A_1\,(\operatorname{sech}[\delta\,(x-x_1)])^{2/p} - A_2\,(\operatorname{sech}[\delta\,(x-x_2)])^{2/p} \tag{19}$$

where amplitude is $A_k = \left(\frac{c_k(p+1)(p+2)}{2\varepsilon}\right)^{1/p}$ $(k = 1,\ 2)$ and $\delta = \sqrt{\frac{p^2}{4\mu}}$. To observe the interaction of the two negative amplitude waves for quartic nonlinearity, the fixed coefficients have been selected as follows $p = 3$, $\varepsilon = 3$, $\mu = 1$, $x_1 = 15$, $x_2 = 30$, $c_1 = 0.3$, $c_2 = 0.0375$. So, the great amplitude value is $A_1 = 1$ chosen and small amplitude value is $A_2 = 0.5$ chosen. Numerical solution investigated over the solution domain [0, 80] and simulation run up to time $t = 100$. The numerical solution is obtained for $\Delta t = 0.05$ and $N = 801$. Numerical invariants are given in Table 13. The three invariants are seen to be nearly unchanged during the simulation. The interaction of the waves is illustrated and given in Figure 8. In Figure 8, the two solitary waves are seen with two

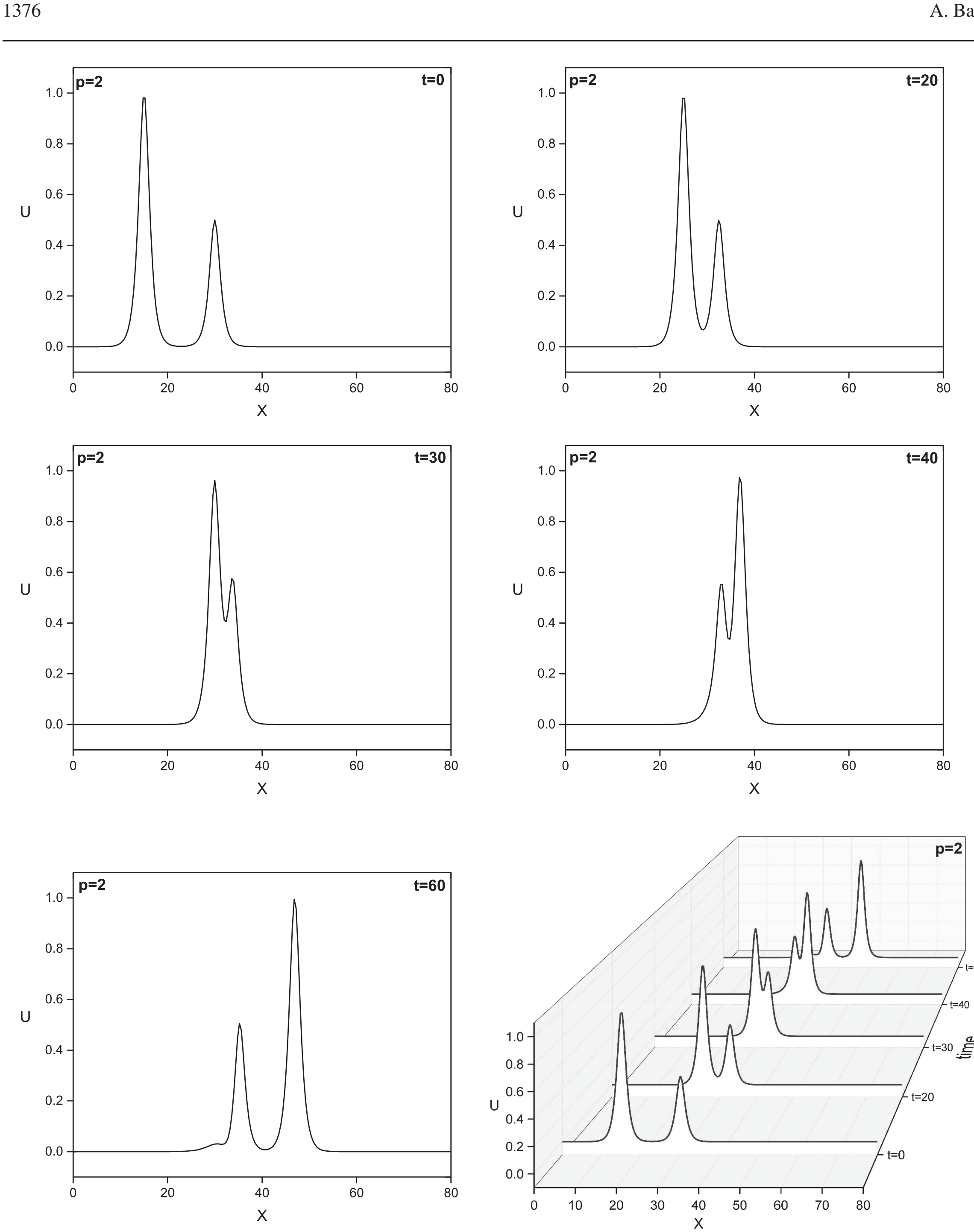

Fig. 4 D.1. Interaction of the two positive amplitude waves for $p = 2$

small wavelets in the final of the run simulation. The present condition is may be explain with the increasing of the order of the nonlinearity.

E.3. Thirdly, numerical solutions of the interaction of the one positive and one negative amplitudes for quartic nonlinear GEW equation is investigated. The condition given at the initial time is selected as follows

$$U(x, 0) = A_1 \left(\operatorname{sec h}\left[\delta\left(x - x_1\right)\right]\right)^{2/p} - A_2 \left(\operatorname{sec h}\left[\delta\left(x - x_2\right)\right]\right)^{2/p} \tag{20}$$

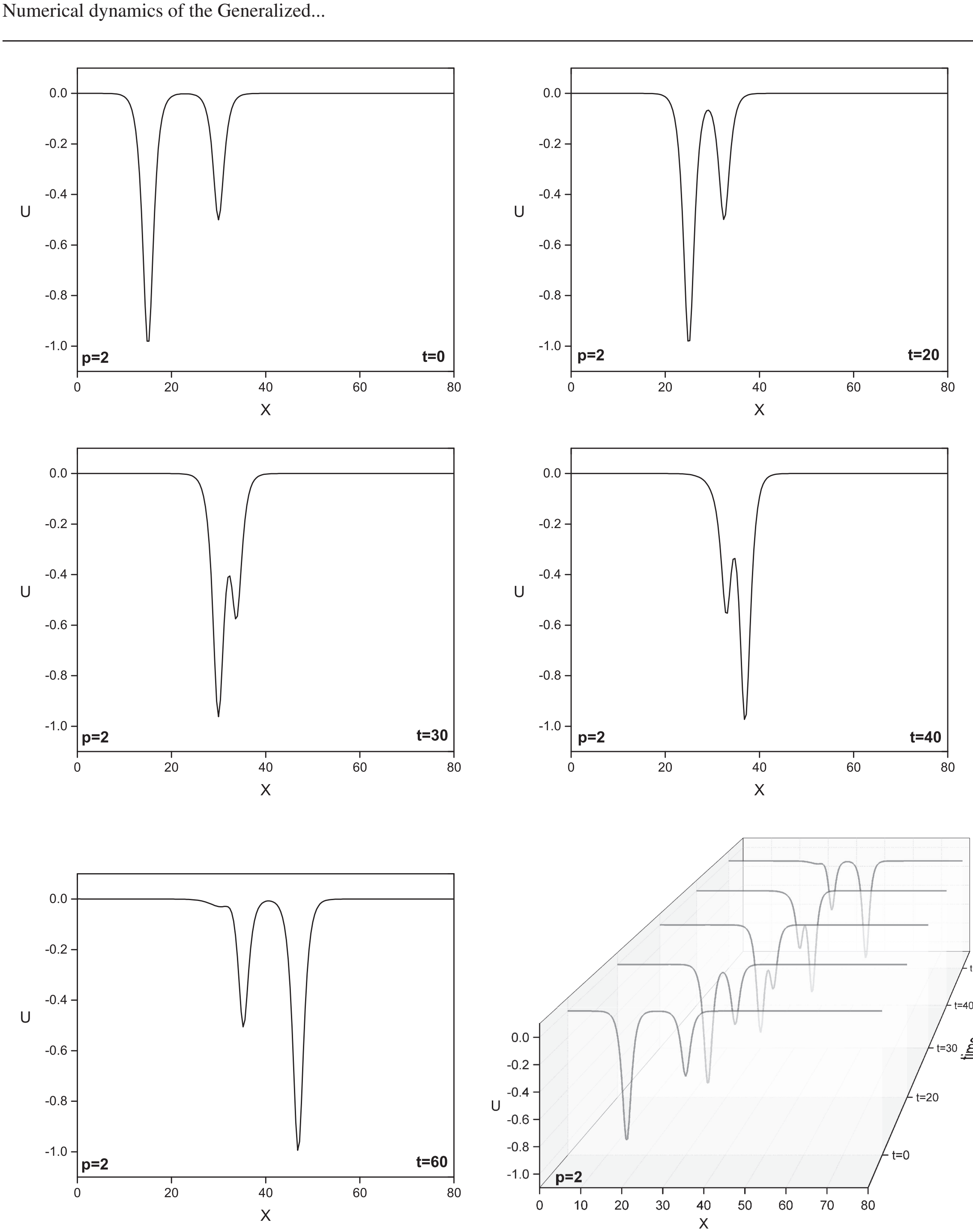

Fig. 5 D.2. The simulation of the interaction between the 2 negative amplitude waves for $p = 2$

where amplitude is $A_k = \left(\frac{c_k(p+1)(p+2)}{2\varepsilon}\right)^{1/p}$ $(k = 1,\ 2)$ and $\delta = \sqrt{\frac{p^2}{4\mu}}$. To observe the interaction of the two positive amplitude waves for quartic nonlinearity, values of the constant parameters are chosen as $p = 3$, $\varepsilon = 3$, $\mu = 1$, $x_1 = 15$, $x_2 = 30$, $c_1 = 0.3$, $c_2 = 0.0375$. So, the great amplitude value is $A_1 = 1$ chosen and small amplitude value is $A_2 = 0.5$ chosen. Numerical solution is investigated over the solution domain [0, 80] and simulation run up to time $t = 100$. The numerical solution is obtained for $\Delta t = 0.05$ and $N = 801$. Numerical invariants are presented in Table 13. The three invariants are seen to be nearly unchanged during the simulation. The interaction of the waves is illustrated and given in Figure 9. In Figure 9, the two solitary waves are seen with

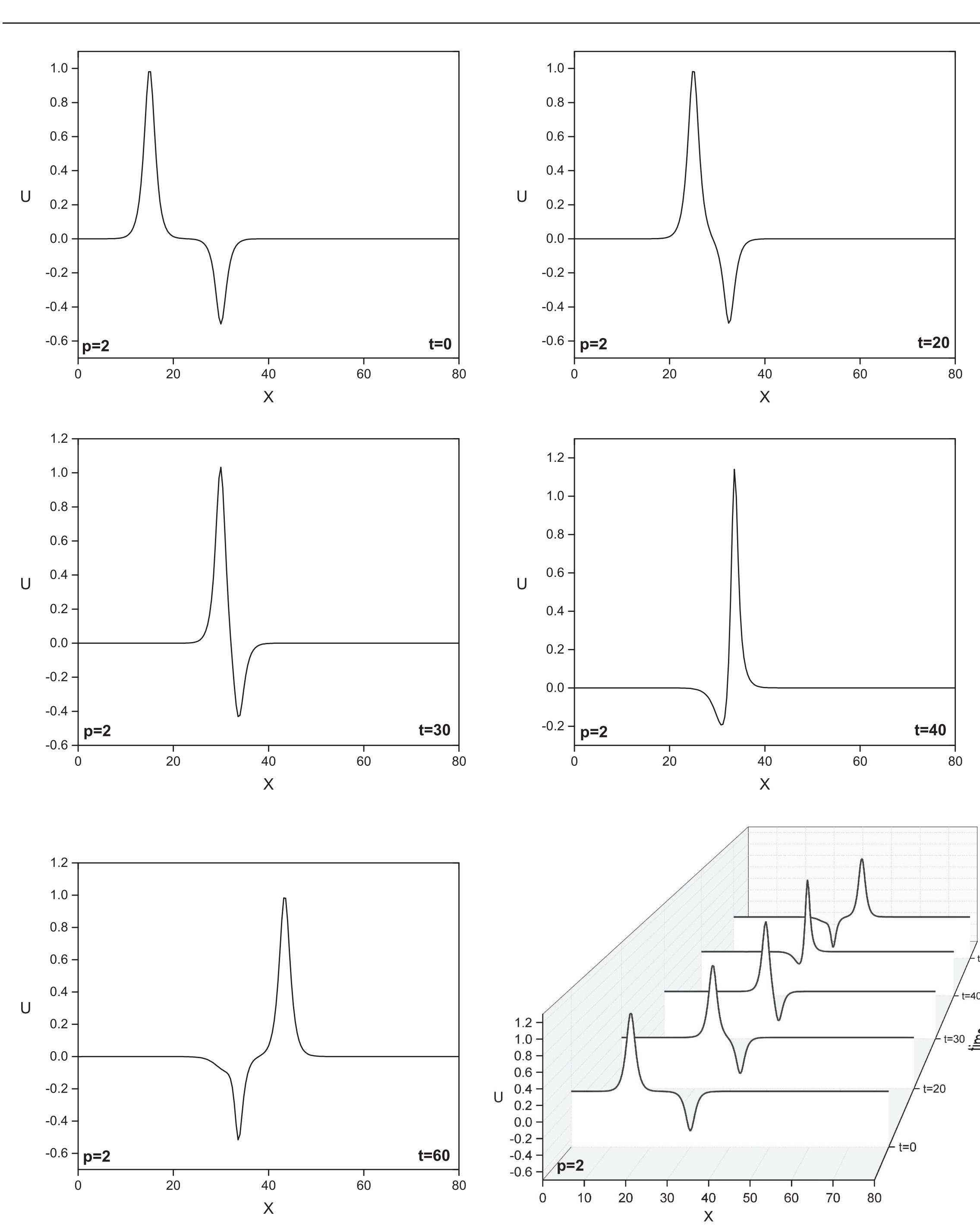

Fig. 6 D.3. The simulation of the interaction between the positive and negative amplitude waves for $p = 2$

two small wavelets in the final of the run simulation. The present condition is may be explain with the increasing of the order of the nonlinearity.

F. In this part, numerical solutions of the interactions of the two different waves for quintic nonlinear GEW equation are investigated.

F.1. Firstly, numerical solution of the interaction of the two positive amplitudes for quintic nonlinear GEW equation is investigated. The condition given at the initial time is selected as follows

$$U(x, 0) = A_1 (\operatorname{sec h} [\delta (x - x_1)])^{2/p} + A_2 (\operatorname{sec h} [\delta (x - x_2)])^{2/p} \tag{21}$$

Table 13 E. The simulation of the interaction between the 2 solitary waves: $p = 3$, $x \in [0, 80]$, $\Delta t = 0.05$, $N = 801$.

	$A_1=1$, $A_2=0.5$			$A_1 = -1$, $A_2 = -0.5$			$A_1=1$, $A_2=-0.5$		
t	I_1	I_2	I_3	I_1	I_2	I_3	I_1	I_2	I_3
0	4.20655	3.07989	1.19186	− 4.20655	3.07989	1.19186	1.40218	3.07989	1.19185
10	4.20643	3.07983	1.19180	− 4.20643	3.07983	1.19180	1.40204	3.07974	1.19174
20	4.20638	3.07988	1.19185	− 4.20638	3.07988	1.19185	1.40195	3.07967	1.19169
30	4.20633	3.07994	1.19190	− 4.20633	3.07994	1.19190	1.40180	3.07966	1.19167
40	4.20620	3.07976	1.19172	− 4.20620	3.07976	1.19172	1.40174	3.07994	1.19183
50	4.20611	3.07986	1.19184	− 4.20611	3.07986	1.19184	1.40166	3.07982	1.19180
60	4.20602	3.07991	1.19189	− 4.20602	3.07991	1.19189	1.40161	3.07985	1.19184
70	4.20596	3.07993	1.19189	− 4.20596	3.07993	1.19189	1.40159	3.07989	1.19189
80	4.20589	3.07994	1.19189	− 4.20589	3.07994	1.19189	1.40153	3.07997	1.19195
90	4.20581	3.07996	1.19190	− 4.20581	3.07996	1.19190	1.40141	3.07987	1.19186
100	4.20570	3.07990	1.19182	− 4.20570	3.07990	1.19182	1.40129	3.07982	1.19182

Table 14 F. Interaction of the two solitary waves: $p = 4$, $x \in [0, 80]$, $\Delta t = 0.05$, $N = 801$.

	$A_1=1$, $A_2=0.5$			$A_1 = -1$, $A_2 = -0.5$			$A_1=1$, $A_2 = -0.5$		
t	I_1	I_2	I_3	I_1	I_2	I_3	I_1	I_2	I_3
0	3.93308	2.94524	1.06250	− 3.93308	2.94524	1.06250	1.31103	2.94524	1.06250
10	3.93304	2.94525	1.06254	− 3.93304	2.94525	1.06254	1.31100	2.94514	1.06246
20	3.93297	2.94529	1.06257	− 3.93297	2.94529	1.06257	1.31093	2.94510	1.06244
30	3.93285	2.94520	1.06249	− 3.93285	2.94520	1.06249	1.31093	2.94526	1.06258
40	3.93281	2.94517	1.06243	− 3.93281	2.94517	1.06243	1.31088	2.94548	1.06272
50	3.93267	2.94519	1.06250	− 3.93267	2.94519	1.06250	1.31079	2.94535	1.06266
60	3.93254	2.94513	1.06243	− 3.93254	2.94513	1.06243	1.31073	2.94536	1.06267
70	3.93244	2.94509	1.06240	− 3.93244	2.94509	1.06240	1.31064	2.94532	1.06264
80	3.93245	2.94522	1.06250	− 3.93245	2.94522	1.06250	1.31056	2.94525	1.06259
90	3.93235	2.94518	1.06248	− 3.93235	2.94518	1.06248	1.31046	2.94523	1.06257
100	3.93234	2.94528	1.06255	− 3.93234	2.94528	1.06255	1.31042	2.94522	1.06257
110	3.93227	2.94529	1.06258	− 3.93227	2.94529	1.06258	1.31032	2.94521	1.06256
120	3.93211	2.94523	1.06254	− 3.93211	2.94523	1.06254	1.31030	2.94523	1.06260

in which amplitude is $A_k = \left(\frac{c_k(p+1)(p+2)}{2\varepsilon}\right)^{1/p}$ $(k = 1,\ 2)$ and $\delta = \sqrt{\frac{p^2}{4\mu}}$. To observe the interaction of the two positive amplitude waves for quintic nonlinearity, the values of the fixed coefficients have been selected as follows $p = 4$, $\varepsilon = 3$, $\mu = 1$, $x_1 = 15$, $x_2 = 30$, $c_1 = 0.2$, $c_2 = 1/80$. So, the great amplitude value is $A_1 = 1$ chosen and small amplitude value is $A_2 = 0.5$ chosen. Numerical solution is investigated over the solution domain [0, 80] and simulation run up to time $t = 120$. The numerical solution is obtained for $\Delta t = 0.05$ and $N = 801$. Numerical invariants are given in Table 14. The calculated invariants seem to be nearly unchanged during the simulation. The interaction of the waves is illustrated and given in Figure 10. In Figure 10, the two solitary waves are seen with two small waves in the final of the run simulation. The present condition may be explained with the increasing of the order of the nonlinearity.

F.2. Secondly, numerical solution of the interaction of the two negative amplitudes for quintic nonlinear GEW equation is investigated. The condition given at the initial time has been chosen as

$$U(x, 0) = -A_1 \left(\operatorname{sech}\left[\delta\left(x - x_1\right)\right]\right)^{2/p} - A_2 \left(\operatorname{sech}\left[\delta\left(x - x_2\right)\right]\right)^{2/p} \tag{22}$$

where amplitude is $A_k = \left(\frac{c_k(p+1)(p+2)}{2\varepsilon}\right)^{1/p}$ $(k = 1,\ 2)$ and $\delta = \sqrt{\frac{p^2}{4\mu}}$. To observe the interaction of the two positive amplitude waves for quintic nonlinearity, the fixed coefficients are selected as follows $p = 4$, $\varepsilon = 3$, $\mu = 1$, $x_1 = 15$, $x_2 = 30$, $c_1 = 0.2$, $c_2 = 1/80$. So, the great amplitude value is $A_1 = 1$ chosen and small amplitude value is $A_2 = 0.5$ chosen. Numerical solution is investigated over the solution domain [0, 80] and simulation run up to time $t = 120$. The numerical solution is obtained for $\Delta t = 0.05$ and $N = 801$. Numerical invariants are given in Table 14. The three invariants are seen to be nearly unchanged during the simulation. The interaction of the waves is illustrated and given in Figure 11. In the figure, the two solitary waves are seen with two small waves in the final of the present simulation. The present condition is may be explain with the increasing of the order of the nonlinearity.

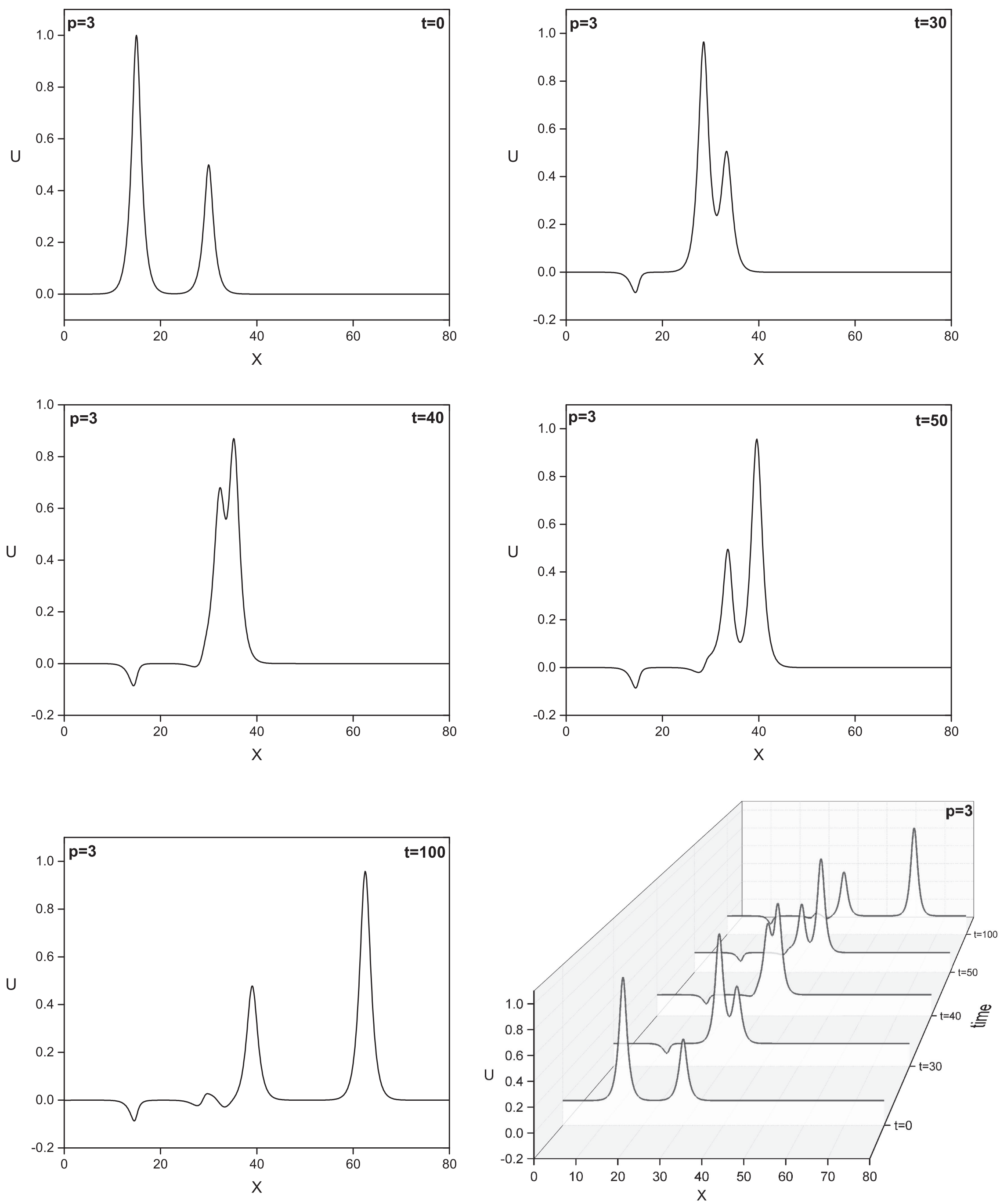

Fig. 7 E.1. Interaction of the two positive amplitude waves for $p = 3$

F.3. Thirdly, numerical solutions of the interaction of the one positive and one negative amplitudes for quintic nonlinear GEW equation is investigated. The initial condition is chosen as

$$U(x, 0) = A_1 \left(\sec\mathrm{h}\left[\delta\left(x - x_1\right)\right]\right)^{2/p} - A_2 \left(\sec\mathrm{h}\left[\delta\left(x - x_2\right)\right]\right)^{2/p} \tag{23}$$

where amplitude is $A_k = \left(\frac{c_k(p+1)(p+2)}{2\varepsilon}\right)^{1/p}$ $(k = 1,\ 2)$ and $\delta = \sqrt{\frac{p^2}{4\mu}}$. To observe the interaction of the two positive amplitude waves for quintic nonlinearity, the fixed coefficients have been selected as follows $\varepsilon = 3$, $\mu = 1$, $x_1 = 15$, $x_2 = 30$, $c_1 = 0.2$, $c_2 = 1/80$. So, the great amplitude value is $A_1 = 1$ chosen and small

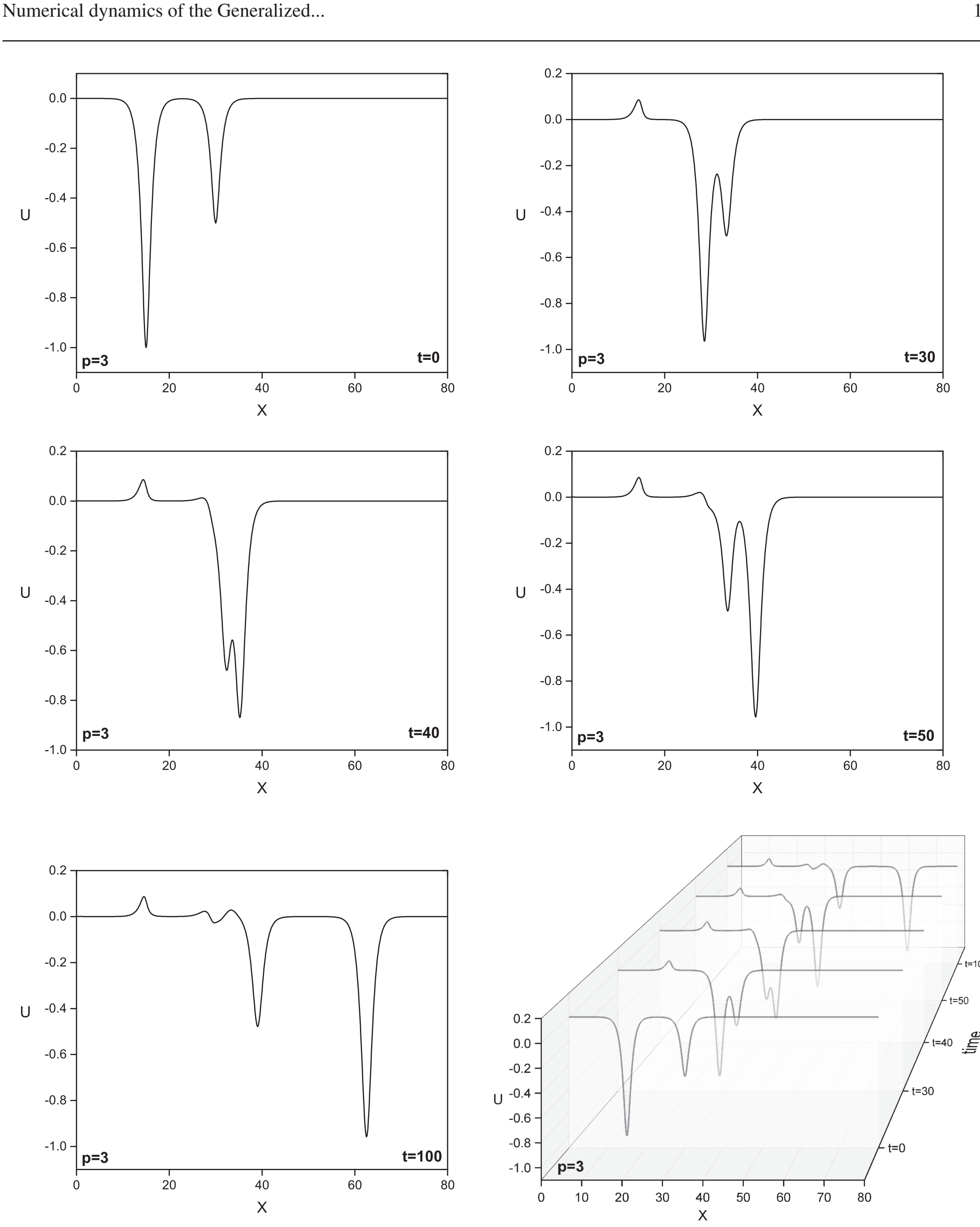

Fig. 8 E.2. The simulation of the interaction between two negative amplitude waves $p = 3$

amplitude value is $A_2 = 0.5$ chosen. Numerical solution is investigated over the solution domain [0, 80] and simulation run up to time $t = 120$. The numerical solution is obtained for $\Delta t = 0.05$ and $N = 801$. Numerical invariants are given in Table 14. The calculated invariants seem to be nearly unchanged during the simulation. The interaction of the waves is illustrated and given in Figure 12. In Figure 12, the two solitary waves are seen with two small waves at the end of the simulation. This situation may be explained with the increasing of the order of the nonlinearity.

Finally, to be able to observe the effect of the high nonlinearity, simulations of the interaction between the 2 solitary waves for different cases are illustrated in Figure 13. For this purpose, time is fixed for all of the cases

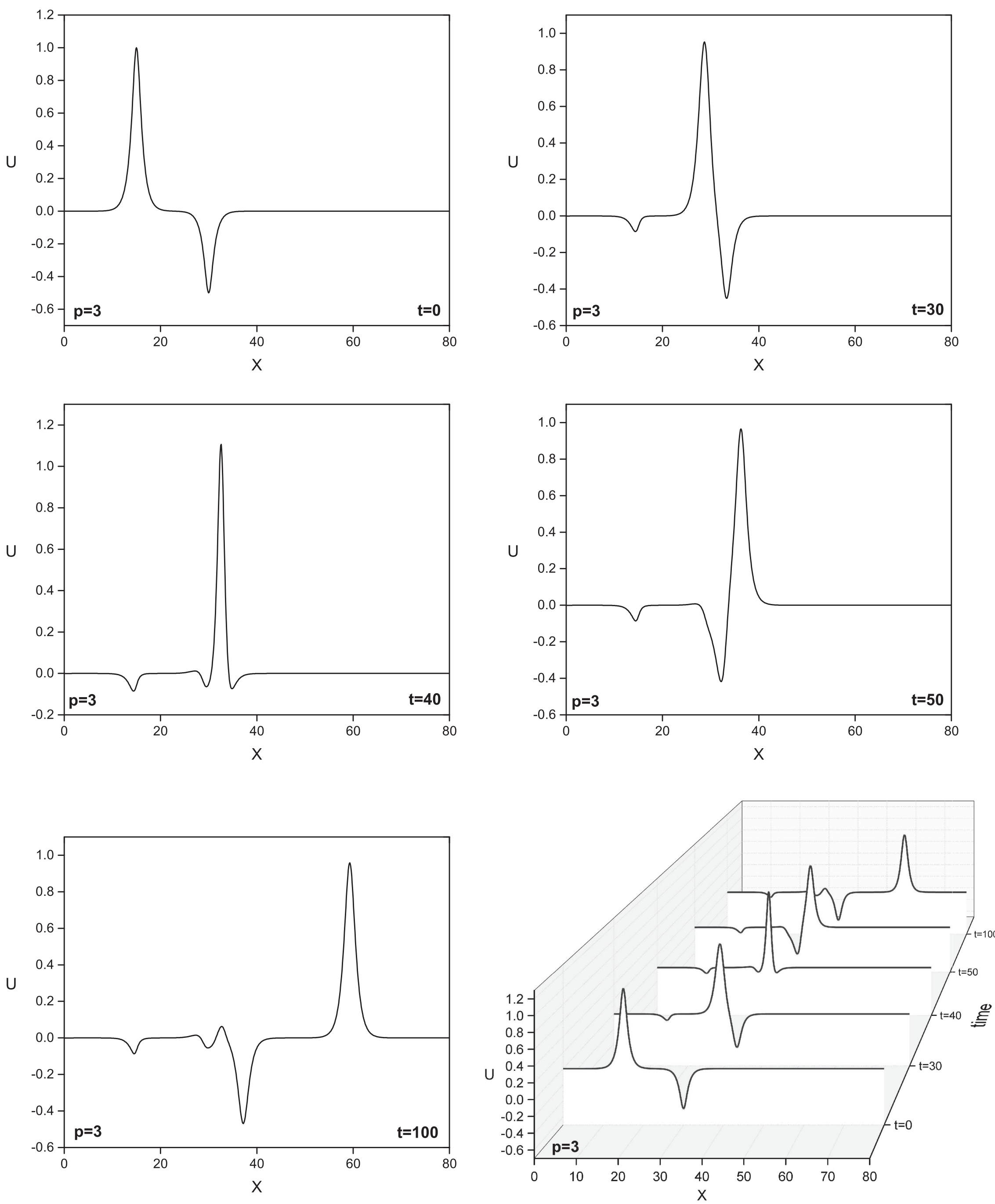

Fig. 9 E.3. Interaction of the one positive and one negative amplitude waves for $p = 3$

at $t = 60$. The positions and amplitudes of the waves for all cases are recorded and given in Table 15. It is clear to see that, by increasing of the nonlinearity, two small waves are occurring at the end of the small wave. For the low-order nonlinear GEW equation, motion of the solitary waves are faster than high-order nonlinear GEW equation. Those results are observed for three different cases and can be clearly seen in Table 15 and in Figure 13. Comparison of the CPU time values for interaction of two solitary waves is given in Table 16.

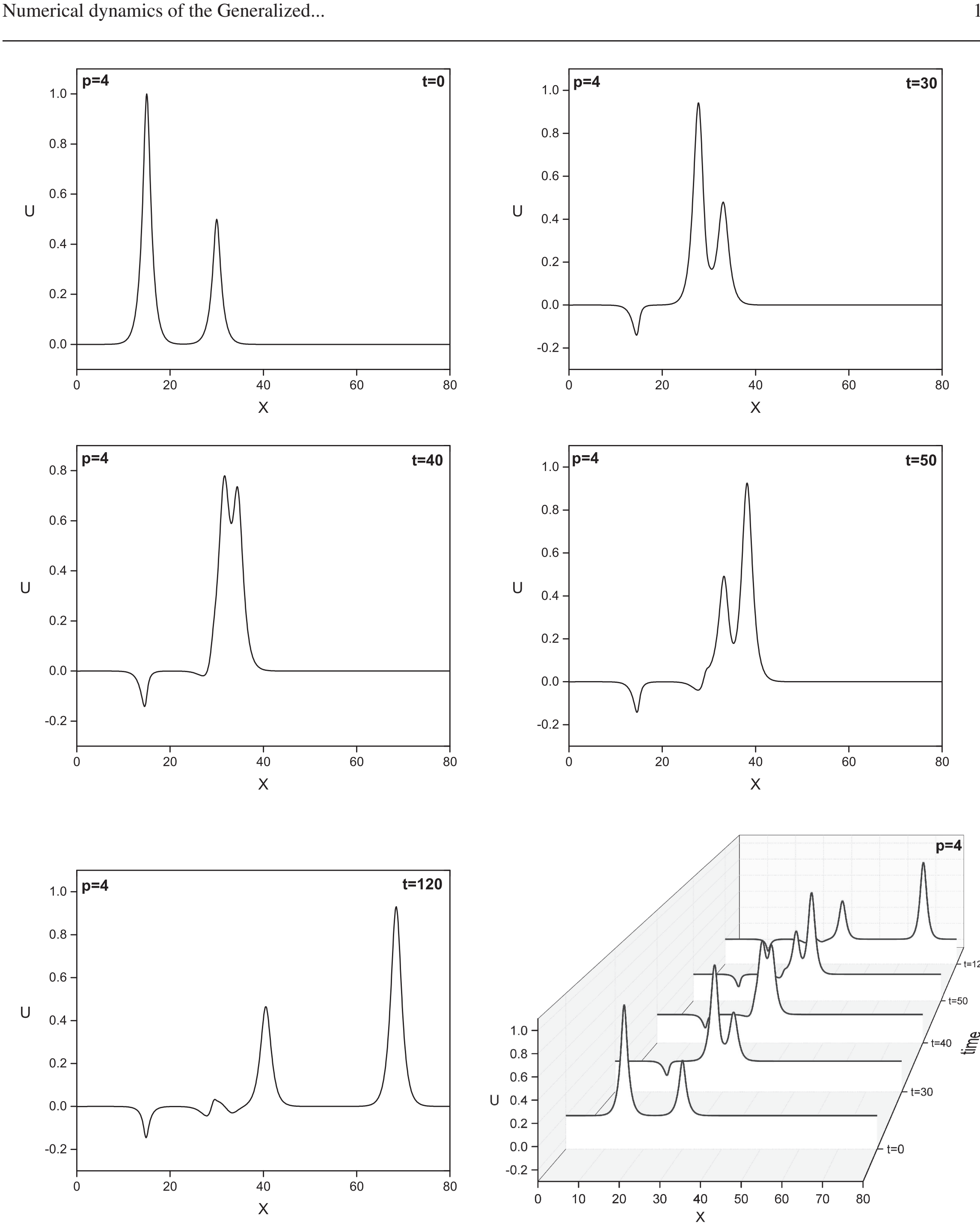

Fig. 10 F.1. Interaction of the two positive amplitude waves for $p = 4$

5 Conclusion

Throughout the present manuscript, high-order nonlinear GEW equation is solved numerically via using mixed method which includes both the differential quadrature and finite difference methods. Single solitary wave solutions for eight different cases and interaction of the two positive amplitude waves, interaction of the two negative amplitude waves and interaction of the one positive and one negative wave solutions for nine different cases are obtained. It is important to note that interaction of the two negative amplitude waves and interaction of the one positive and one negative wave solutions of the high-order GEW equation are firstly in

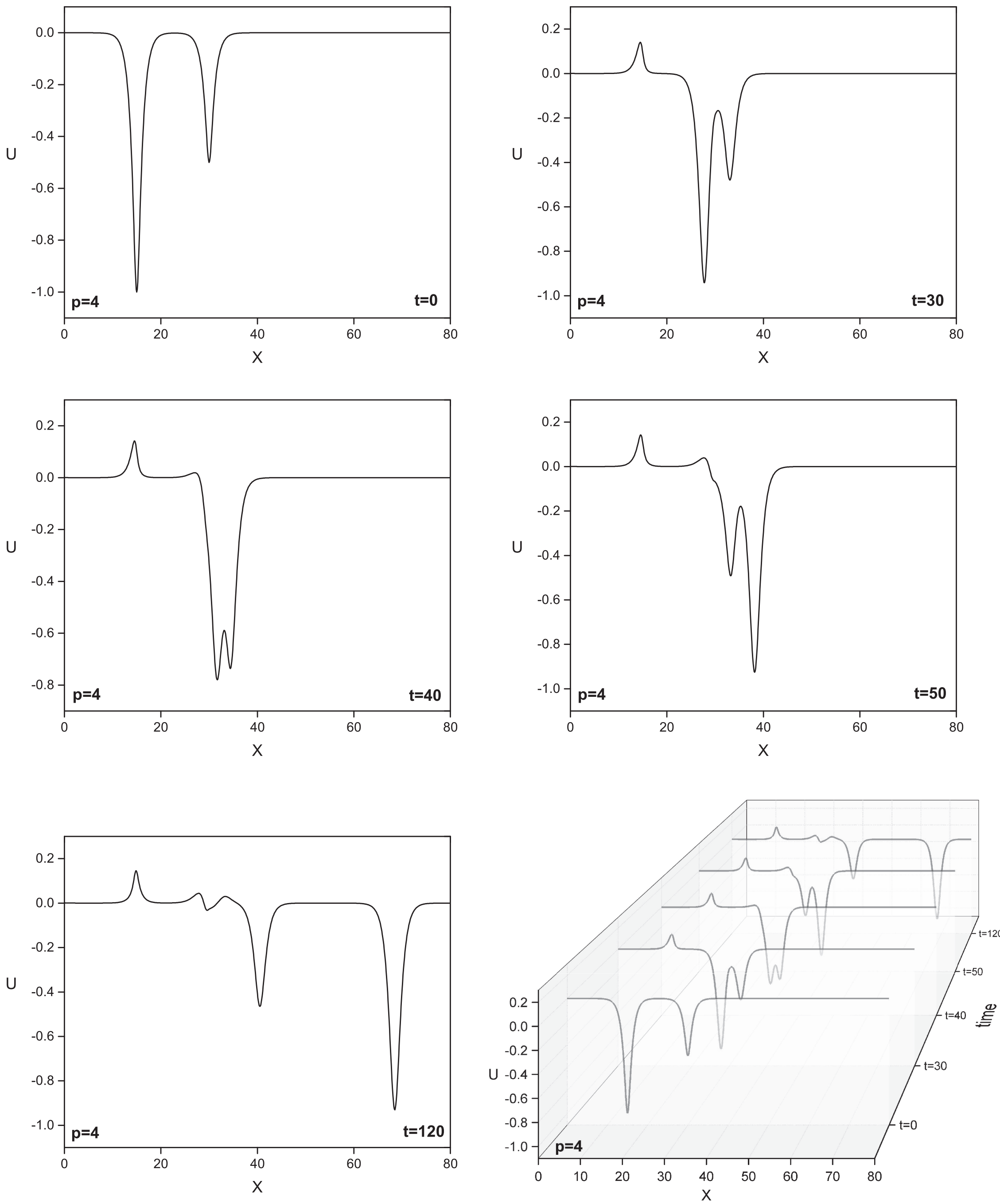

Fig. 11 F.2. The simulation for the interaction between two negative amplitude waves for $p = 4$

this study examined. To be able to see clearly the performance of the present mixed method error norms and conservative quantities are calculated and compared with earlier studies. The contribution of the newly presented mixed method can easily be observed with comparisons. Also, the effect of the nonlinearity is observed with comparison of the different order GEW equation solutions. As a conclusion, the newly presented mixed method can be utilized for future studies including high-order nonlinear differential equation.

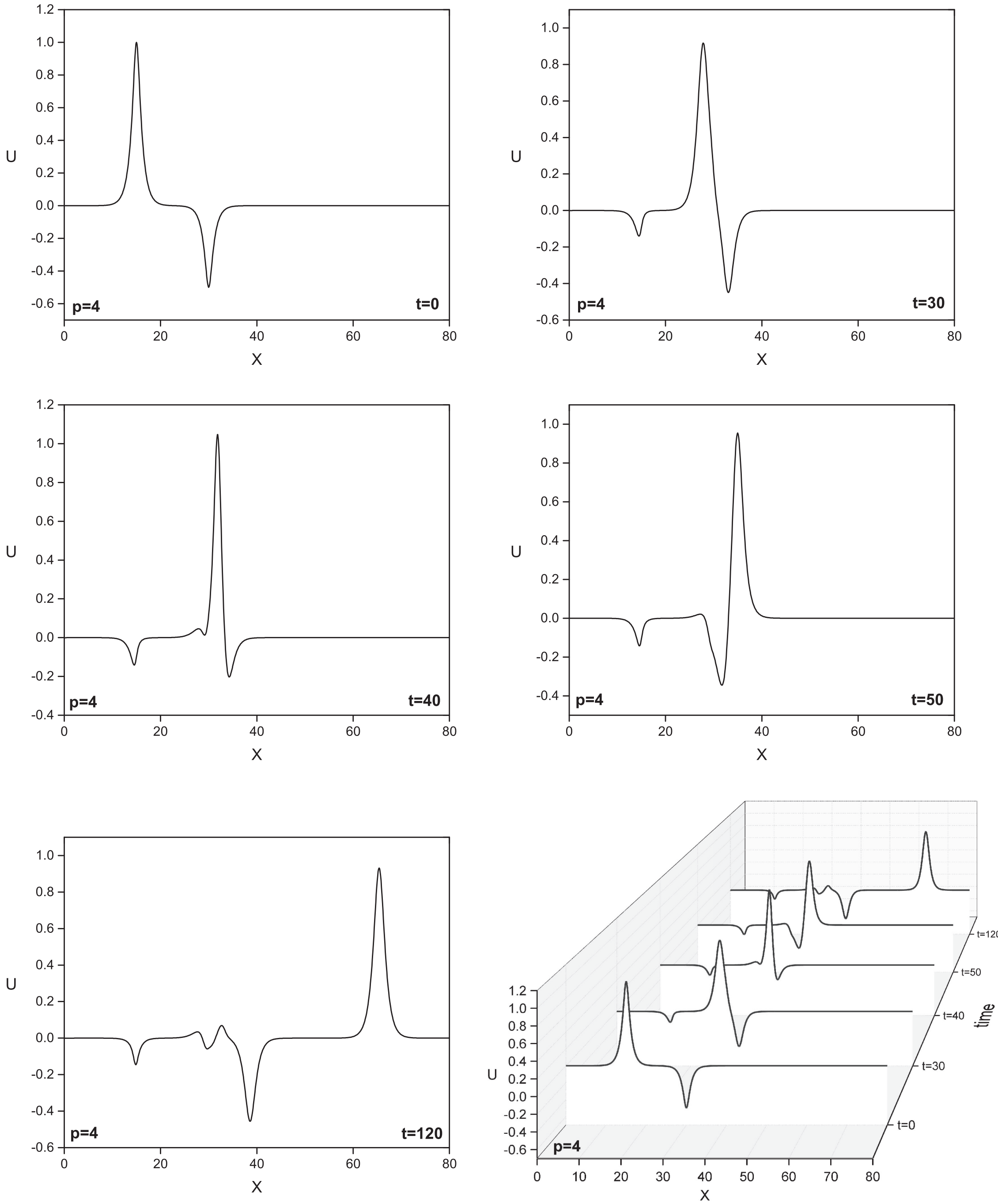

Fig. 12 F.3. The simulation of the interaction between positive and negative amplitude waves for $p = 4$

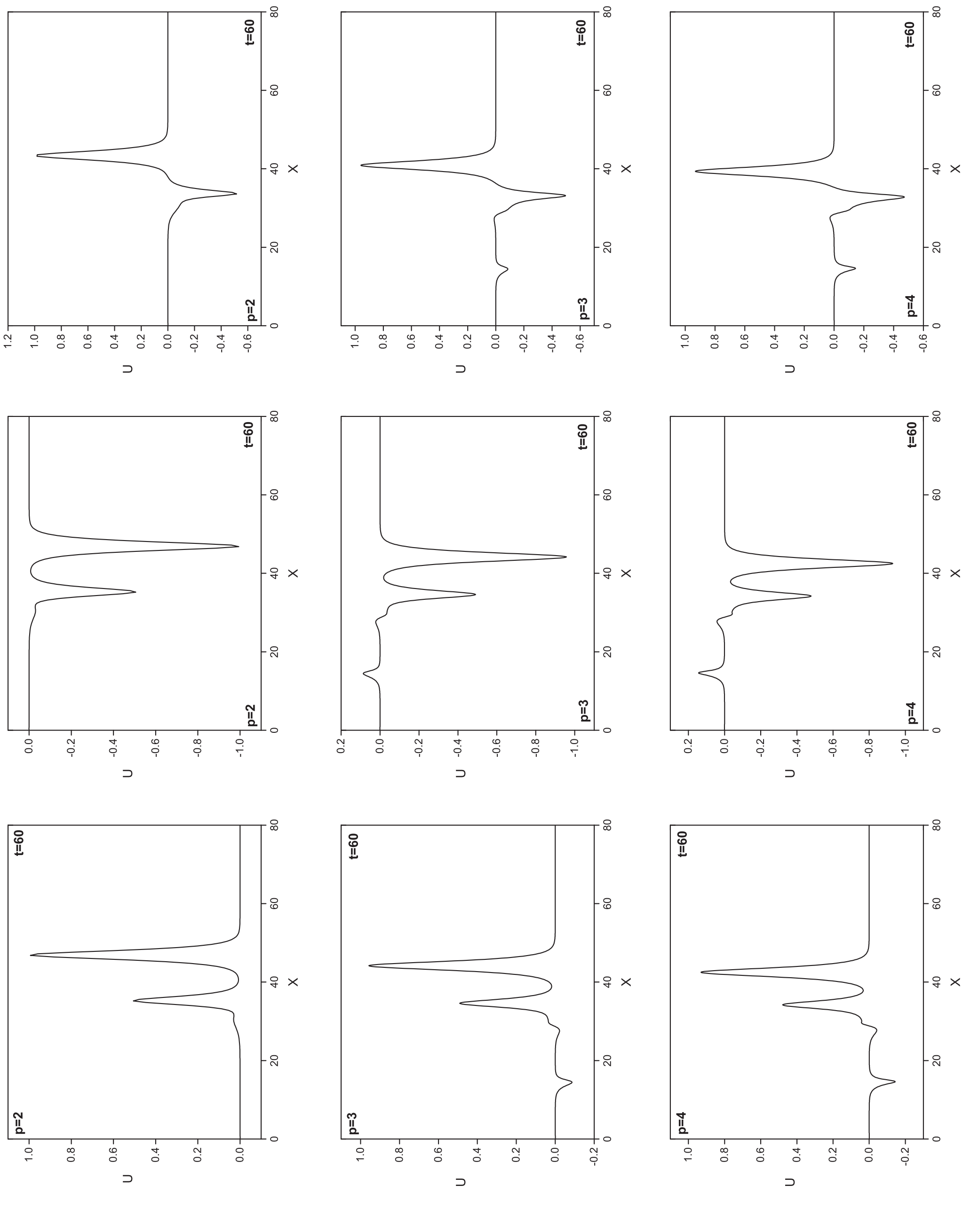

Fig. 13 D., E., F. The effect of the nonlinearity order for $p = 2, 3$ and 4 , respectively

Table 15 D., E., F. The effect of the nonlinearity order to motion and amplitudes

		Two positive				Two negative				One positive and one negative			
p	t	x_1	x_2	U_1	U_2	x_1	x_2	U_1	U_2	x_1	x_2	U_1	U_2
2	0	15.0	30.0	1.00000	0.50000	15.0	30.0	− 1.00000	− 0.50000	15.0	30.0	1.00000	− 0.50000
	60	46.8	35.2	0.99407	0.50550	46.8	35.2	− 0.99407	− 0.50550	43.2	33.6	0.98262	− 0.51621
3	0	15.0	30.0	1.00000	0.50000	15.0	30.0	− 1.00000	− 0.50000	15.0	30.0	1.00000	− 0.50000
	60	44.2	34.6	0.95756	0.49057	44.2	34.6	− 0.95756	− 0.49057	40.9	33.2	0.95916	− 0.49586
4	0	15.0	30.0	1.00000	0.50000	15.0	30.0	− 1.00000	− 0.50000	15.0	30.0	1.00000	− 0.50000
	60	42.5	34.2	0.93046	0.47882	42.5	34.2	− 0.93046	− 0.47882	39.4	32.8	0.93163	− 0.47204

Table 16 D, E, F. Comparison of the CPU time values for interaction of two solitary waves

p	c_1	c_2	A_1	A_2	Δt	N	T_{Final}	CPU time (sec.)
2	0.5	0.125	1	0.5	0.2	201	60	76.719
3	0.3	0.0375	1	0.5	0.2	201	60	75.828
4	0.2	1/80	1	0.5	0.2	201	60	75.859
2	0.5	0.125	1	0.5	0.2	401	60	582.281
3	0.3	0.0375	1	0.5	0.2	401	60	576.641
4	0.2	1/80	1	0.5	0.2	401	60	575.484
2	0.5	0.125	1	0.5	0.2	601	60	2001.531
3	0.3	0.0375	1	0.5	0.2	601	60	2053.953
4	0.2	1/80	1	0.5	0.2	601	60	2036.000
2	0.5	0.125	1	0.5	0.2	801	60	4793.188
3	0.3	0.0375	1	0.5	0.2	801	60	4857.984
4	0.2	1/80	1	0.5	0.2	801	60	4866.641

Acknowledgements The author expresses his deep gratitude to editor-in-chief, his staff and anonymous referees for their invaluable contributions to a better content and reading of the manuscript.

Data Availibility Statement The numerical data obtained for this article are available from the corresponding author, upon reasonable request.

Declarations

Conflict of interest The author states that there is no conflict of interest.

References

1. Başhan, A.: Modification of quintic B-spline differential quadrature method to nonlinear Korteweg-de Vries equation and numerical experiments. Applied Numerical Mathematics. **167,** 356–374 (2021) https://doi.org/10.1016/j.apnum.2021.05.015
2. Başhan, A.: A numerical treatment of the coupled viscous Burgers' equation in the presence of very large Reynolds number. Physica A. **545,** 123755 (2020) https://doi.org/10.1016/j.physa.2019.123755
3. Başhan, A.: A mixed algorithm for numerical computation of soliton solutions of the coupled KdV equation: Finite difference method and differential quadrature method, Applied Mathematics and Computation. **360**, 42-57 (2019) https://doi.org/10.1016/j.amc.2019.04.073
4. Başhan, A., Esen, A.: Single soliton and double soliton solutions of the quadratic-nonlinear Korteweg-de Vries equation for small and long-times. Numer Methods Partial Differential Eq. **37**, 1561–1582 (2021) https://doi.org/10.1002/num.22597
5. Başhan, A., Uçar, Y., Yağmurlu, N.M., Esen, A.: Numerical solutions for the fourth order extended Fisher-Kolmogorov equation with high accuracy by differential quadrature method. Sigma J Eng & Nat Sci. **9** (3) 273-284 (2018)
6. Başhan, A., Yağmurlu, N.M., Uçar, Y., Esen, A.: An effective approach to numerical soliton solutions for the Schrödinger equation via modified cubic B-spline differential quadrature method. Chaos, Solitons and Fractals. **100**, 45-56 (2017) https://doi.org/10.1016/j.chaos.2017.04.038
7. Başhan, A., Yağmurlu, N.M., Uçar, Y., Esen, A.: Finite difference method combined with differential quadrature method for numerical computation of the modified equal width wave equation. Numer Methods Partial Differential Eq. **37**, 690-706 (2021) https://doi.org/10.1002/num.22547
8. Bellman, R., Kashef, B.G., Casti, J.: Differential quadrature: a tecnique for the rapid solution of nonlinear differential equations. Journal of Computational Physics. **10,** 40-52 (1972) https://doi.org/10.1016/0021-9991(72)90089-7
9. Evans, D.J., Raslan, K.R.: Solitary waves for the generalized equal width (GEW) equation, International Journal of Computer Mathematics. **82**, 445-455 (2005) https://doi.org/10.1080/0020716042000272539

10. Hamdi, S., Enright,W.H., Schiesser,W.E., Gottlieb, J.J.: Exact Solutions of the Generalized Equal Width Wave Equation, ICCSA 2003, LNCS 2668, 725–734 (2003) https://doi.org/10.1007/3-540-44843-8_79
11. Hamdi, S., Enright,W.H., Schiesser,W.E., Gottlieb, J.J.: Exact solutions and invariants of motion for general types of regularized long wave equations. Mathematics and Computers in Simulation. **65**, 535–545 (2004) https://doi.org/10.1016/j.matcom.2004.01.015
12. İnan, B., Bahadır, A.R.: A Fully Implicit Finite Difference Approach for Numerical Solution of the Generalized Equal Width (GEW) Equation*,* Proc. Natl. Acad. Sci., India, Sect. A Phys. Sci. **90**(2) 299-308 (2020) https://doi.org/10.1007/s40010-019-00594-8
13. Karakoç, S.B.G.: A numerical analysing of the GEW equation using finite element method: Journal of Science and Arts. **2**(47), 339-348 (2019)
14. Karakoç, S.B.G., Omrani, K., Sucu, D.: Numerical investigations of shallow water waves via generalized equal width (GEW) equation. Applied Numerical Mathematics. **162**, 249–264 (2021) https://doi.org/10.1016/j.apnum.2020.12.025
15. Karakoç, S.B.G., Zeybek, H.: A cubic B-spline Galerkin approach for the numerical simulation of the GEW equation. Stat., Optim. Inf. Comput., **4,** 30–41 (2016)
16. Karakoç, S.B.G., Zeybek, H.: A septic B-spline collocation method for solving the generalized equal width wave equation. Kuwait J. Sci. **43** (3), 20-31 (2016)
17. Morrison, P.J., Meiss, J.D., Cary, J.R.: Scattering of RLW solitary waves. Physica D. **11,** 324–336 (1984) https://doi.org/10.1016/0167-2789(84)90014-9
18. Olver, P.J.: Euler operators and conservation laws of the BBM equation. Math Proc. Camb. Phil. Soc., **85**, 143-160 (1979) https://doi.org/10.1017/S0305004100055572
19. Oruç, Ö.: Delta-shaped basis functions-pseudospectral method for numerical investigation of nonlinear generalized equal width equation in shallow water waves, Wave Motion. **101,** 102687 (2021) https://doi.org/10.1016/j.wavemoti.2020.102687
20. Prenter, P.M.: *Splines and Variational Methods, John Wiley, New York*, 1975.
21. Raslan, K.R.: Collocation method using cubic B-spline for the generalised equal width equation, Int. J. Simulation and Process Modelling, **2**(1/2), 37-44 (2006)
22. Roshan, T.: A Petrov–Galerkin method for solving the generalized equal width (GEW) equation. Journal of Computational and Applied Mathematics. **235,** 1641–1652 (2011) https://doi.org/10.1016/j.cam.2010.09.006
23. Rubin, S.G., Graves, R.A.: A cubic spline approximation for problems in fluid mechanics, (National aeronautics and space administration,Technical Report, Washington, (1975)
24. Shu, C.: *Differential Quadrature and its application in engineering, Springer-Verlag London Ltd.*, (2000)
25. Taghizadeh, N., Mirzazadeh, M. Akbari, M., Rahimian, M.: Exact Soliton Solutions for Generalized Equal Width Equation, Math. Sci. Lett. **2**(2), 99-106 (2013) https://doi.org/10.12785/msl/020204
26. Yağmurlu, N.M., Karakaş, A.S.: Numerical solutions of the equal width equation by trigonometric cubic B-spline collocation method based on Rubin-Graves type linearization. Numer Methods Partial Differential Eq. **36**, 1170-1183 (2020) https://doi.org/10.1002/num.22470
27. Zeybek, H., Karakoç, S.B.G.: Application of the collocation method with B-splines to the GEW equation. Electronic Transactions on Numerical Analysis. **46**, 71–88 (2017)